Dalton Transactions

Accepted Manuscript

ROYAL SOCIETY OF CHEMISTRY

www.rsc.org/dalton

Journal Name

ARTICLE

Synthesis and characterization of polyborosilazane/Cp_2ZrCl_2 hybrid precursor for Si-B-C-N-Zr multinary ceramic

Received 00th January 20xx,
Accepted 00th January 20xx

DOI: 10.1039/x0xx00000x

www.rsc.org/

Xin Long*, Changwei Shao, Hao Wang and Jun Wang

Novel zirconium-contained polyborosilazane (PBSZ-Zr) was synthesized by chemical modification of a liquid polyborosilazane (LPBSZ) with Cp_2ZrCl_2. Si-B-C-N-Zr multinary ceramic was prepared via pyrolysis of PBSZ-Zr. The properties and the ceramization process of PBSZ-Zr, as well as the microstructural development and properties of derived SiBCN-Zr ceramic, were well studied. The active Si-H and N-H groups in LPBSZ react with the Zr-Cl in Cp_2ZrCl_2 to form PBSZ-Zr polymer, The Zr content of SiBCN-Zr ceramic was 3.39 wt % when the weight ratio of Cp_2ZrCl_2 to LPBSZ was 20:100. SiBCN-Zr ceramic remains amorphous when pyrolyzed below 1600 °C, but the crystal phases of Zr_2CN, ZrC, BN, SiC, and Si_3N_4 were detected from 1600 °C treated sample. Due to the low activity of free carbon at the interface of SiBCN-Zr ceramic, the oxidation resistance of SiBCN-Zr ceramic under air was improved compared with SiBCN ceramic.

Introduction

With more and more strict requirements for the rate of hypersonic flight vehicles, ultra-high-temperature ceramics with excellent thermal stability, mechanical strength and resistance to oxidation at a very high temperature are highly needed [1–6]. Carbide, nitride, boride of refractory mental (such as Zr, Hf and Ta) as well as their composite ceramics are all called ultra-high-temperature ceramics, and all of the ceramics have melting points above 3000 °C. The single phase ultra-high-temperature ceramics, such as ZrC and ZrB_2 with low density, high strength, high modulus and excellent resistance to high temperature, have been applied in a lot of areas [7]. However, single phase ZrC and ZrB_2 ceramics have the weak fracture toughness and unsatisfactory resistance to oxidation at high temperature. Furthermore, the difficulty to densify ceramic makes the fabrication cost very high [8, 9]. In order to improve the oxidation resistance and reduce the fabrication cost of single phase ceramics, multinary ceramics, such as ZrB_2-SiC, ZrB_2-Si_3N_4, ZrB_2-SiC-ZrC, ZrB_2-SiC-C and ZrB_2-SiC-BN, have become a hot research topic and achieved some progress recently [1–3,10].

Studies have proved that multinary ceramics are more superior to single phase ceramics [10–15]. Bartuli found that the formation of $ZrSiO_4$ phase in the ZrB_2-SiC surface can well enhance the burning erosion resistance and high temperature oxidation resistance, and the linear ablative of ZrB_2-SiC ceramic is 0.001 mm/s at 2800 °C [12]. Li discovered that ZrB_2-SiC-BN has a better fracture toughness property due to the formation of BN nanocrystals. The BN nanocrystals, with a certain length to diameter ratio, can formed the weak interface with ceramic matrix to well absorb the energy from the crack extension [15]. At present, the fabrication methods of multinary ultra-high-temperature ceramics are limited in hot pressed sintering, pressureless sintering, spark plasma sintering and so on. However, all of these methods are difficult to prepare final products with homogeneous and stable structure, and the cost is also too high. Polymer-derived ceramic method is superior in fabrication of ultra-high-temperature ceramics with low sintering temperature and easy densifying process [16–20]. Thus, by polymer-derived method, compacted and homogeneous ceramics can be prepare easily with a rather low cost.

In our work, a new kind of hybrid preceramic polymer (PBSZ/Cp_2ZrCl_2) was synthesized by one step thermopolymerization of liquid polyborosilazane (PBSZ) and Cp_2ZrCl_2. A novel Si-B-N-C-Zr multinary ceramic was obtained by pyrolysis of PBSZ/Cp_2ZrCl_2. This work provided a polymer-derived ceramic method for synthesis of Si-B-N-C-Zr ceramic, which could be easily applied in the synthesis of Si-B-N-C-Hf, Si-B-N-C-Ta and other multinary ceramics.

Experimental

General

All reactions were conducted under dry N_2 atmosphere by using Schlenk techniques. Liquid polyborosilazane (LPBSZ) with a number average molecular weight of ca. 900 and a polydispersity index of 1.43 was prepared by a one-pot synthesis method of BCl_3, Cl_2SiHCH_3, and $(CH_3)_3SiNHSi(CH_3)_3$ as the starting materials [21]. Cp_2ZrCl_2 was purchased from Alfa Aesar Ltd. in Tianjing, China, and stored in an argon glove box until used.

[a] Science and Technology on Advanced Ceramic Fibers and Composites Laboratory, College of Aerospace Science and Engineering, National University of Defense Technology, Changsha 410073, PR China. E-mail: longxinnudt@163.com

Characterization

The oxygen and nitrogen content of PBSZ/Cp_2ZrCl_2 hybrid precursor as well as the Si-B-N-C-Zr ceramic was determined by a Horiba Oxygen/Nitrogen Analyzer EMIA-820 (Horiba, Japan), and a Horiba Carbon/Sulfur Analyzer EMIA-320V for the content of carbon. The content of silicon in the samples was determined utilizing alkali fusion method. The zirconium content was determined using Vista-MPX inductively coupled plasma emission spectrometry (Variant, America). The X-ray photoelectron spectroscopy (XPS) spectra were examined by an Escalab 250Xi electron spectrometer (Thermo Scientific, USA) using Al Kα radiation. FT-IR spectra were obtained with a Nicolet Avator 360 apparatus (Nicolet, America) using KBr pellets, and the spectras were collected from wavenumbers 400–4000 cm^{-1}. ^{13}C nuclear magnetic resonance (^{13}C NMR) data was gathered with a Bruker AV-400 spectrometer (Bruker, Germany) operating at 75.46 MHz. The samples were dissolved in $CDCl_3$ solution, and the chemical shifts were referred to tetramethylsilane (TMS) (assigned to 0 ppm). The polymer-to-ceramic transformation of PBSZ/Cp_2ZrCl_2 hybrid precursor was studied by means of TGA/MS on a thermal analysis device (TGA/DSC 2 METTLER TOLEDO, Switzerland) coupled with a mass spectrometer (QMG700, INFICON, Germany). Solid-state ^{29}Si-magic angle spinning nuclear magnetic resonance (^{29}Si MAS NMR) experiments were performed on a Bruker AV 300 NMR spectrometer. The samples were spun at 5.0 kHz and the ^{29}Si isotropic chemical shifts were referenced to tetramethylsilane. X-ray diffraction (XRD) studies were carried out with a Bruker AXS D8 Advance diffractometer (Bruker, Germany) with Cu Kα radiation (k = 1.54178 A°). The specimens were continuously scanned from 10° to 90° at a speed of 0.0167 °/s. The morphology of the samples was examined with a scanning electron microscope (SEM; HITACHI S-4800, Japan). The elemental analysis of the ceramics surface was performed by an energy dispersive spectrometer (EDS; HITACHI S-4800, Japan). For transmission electron microscopy (TEM), the powdered samples were dispersed in alcohol by ultrasonicating for 10 min and a drop of the dispersed solution was deposited on a 3 mm carbon-coated copper grid. TEM and high resolution TEM (HR-TEM) images were taken using JEOL 100CX Ⅱ (USA), with an accelerating voltage of 200 kV by using finely pulverized samples. For oxidation resistance test, the ceramic pyrolyzed at 1600 °C were put into a molybdenum disilicide element box furnace and heated at 1550 °C for 1 h in ambient air. The heating rate was 20 °C /min.

Synthesis of polymers

Synthesis of PBSZ/Cp_2ZrCl_2 hybrid precursor was carried out in a Schlenk flask with a magnetic stirrer, a thermocouple and a N_2 inlet. Firstly, 2.5 g Cp_2ZrCl_2 was added into a 250 mL Schlenk flask at room temperature. The flask was dried with flowed dry N_2 gas at 120 °C before used. Secondly, 50.0 g LPBSZ was added into the flask to mix with Cp_2ZrCl_2 in a nitrogen atmosphere. The mixture was heated at 170 °C for 6 hours in a flowed nitrogen atmosphere to form a light yellow liquid. For further polymerization, the light yellow liquid was heated at 190 °C for 4 hours, following a heating time of 4 hours at 230 °C and 4 hours at 250 °C. The final product was light yellow, rubbery solid at room temperature, named as PBSZ-Zr5. The other samples were synthesized by using the same method but with different weight of Cp_2ZrCl_2 to LPBSZ. The weight ratio of Cp_2ZrCl_2 to LPBSZ was varied from 0:100, 5:100, 10:100 to 20:100, and the samples were abbreviated as PBSZ, PBSZ-Zr5, PBSZ-Zr10 and PBSZ-Zr20, correspondingly.

Pyrolysis of polymers

With the pyrolysis temperatures below 1000 °C, the samples were put into an alumina boat and heated in a tube furnace under a N_2 flow. For the pyrolysis temperatures above 1000 °C, the sample was put in a graphite crucible and heated in a vacuum furnace in argon atmosphere. The temperature was progressively rose to 300 °C at a rate of 5 °C/min. After holding at 300 °C for 1 hour, the temperature went on increasing (heating rate: 5 °C/min below 1000 °C, 20 °C/min above 1000 °C) until the pyrolysis temperature was reached. Then the samples were kept at the pyrolysis temperature for 2 hours, and furnace-cooled to RT at last. PBSZ, PBSZ-Zr5, PBSZ-Zr10 and PBSZ-Zr20 derived ceramic upon pyrolysis at high temperature were named as SiBCN, SiBCN-Zr5, SiBCN-Zr10 and SiBCN-Zr20, correspondingly.

Results and discussion

The chemical composition of PBSZ/Cp_2ZrCl_2 hybrid precursor was determined by bulk chemical analysis, and the results are shown in Table 1. Zirconium and carbon content in the precursor increased with the weight ratio of Cp_2ZrCl_2 to PBSZ increasing because higher amount of Cp_2ZrCl_2 was introduced into the hybrid precursor. The Zr content in the hybrid precursor is a little bit lower than theoretical results, because some Cp_2ZrCl_2 was sublimed during the synthesis process, and as the Zr content increasing, the discrepancy increases.

Table 1 Chemical composition of PBSZ/Cp_2ZrCl_2 hybrid precursor from bulk chemical analysis.

Sample	Chemical analysis (wt %)					
	Si	B	N	C	Zr	O
PBSZ	18.7	7.1	36.5	32.9	0	2.3
PBSZ-Zr5	23.7	7.0	30.2	32.8	1.5	2.6
PBSZ-Zr10	21.8	4.8	28.8	35.4	2.0	2.0
PBSZ-Zr20	20.7	4.0	27.5	40.4	4.2	1.7

Simulation of the XPS graphs of PBSZ-Zr10 (Fig. 1) reveals that, the Si_{2p} elemental peak shows two major sharp peaks corresponding to Si-N type bond (101.9 eV) and Si-C type bond (101.0 eV) [22], with a smaller peak at a higher energy of 102.8 eV due to Si-O bond. The B_{1s} valence elemental peak can be clearly divided into two parts, B-N and B-O type bonds at ~190.3 and 192.6 eV, respectively. The XPS spectra of Zr_{3d} in PBSZ-Zr10 and Cp_2ZrCl_2 are quite different. The XPS spectrum from Cp_2ZrCl_2 suggests a strong peak for Zr-Cl (182.3 eV), a low

energy peak for Zr-Cp (180.2 eV) and a higher energy peak for $Zr_{3d3/2}$ (184.6 eV). As for XPS spectrum from PBSZ-Zr10, the Zr-Cl peak disappeared, and two new bonds of Zr-N (182.4 eV) and Zr-Si (181.6 eV) were found, while the peak for Zr-Cp and $Zr_{3d3/2}$ almost remain unchanged. So in this way, we hypothesize the reaction mechanism as scheme 1. Herein, The Si-H and N-H groups in LPBSZ provide the reactive groups to react with the Zr-Cl bond in Cp_2ZrCl_2.

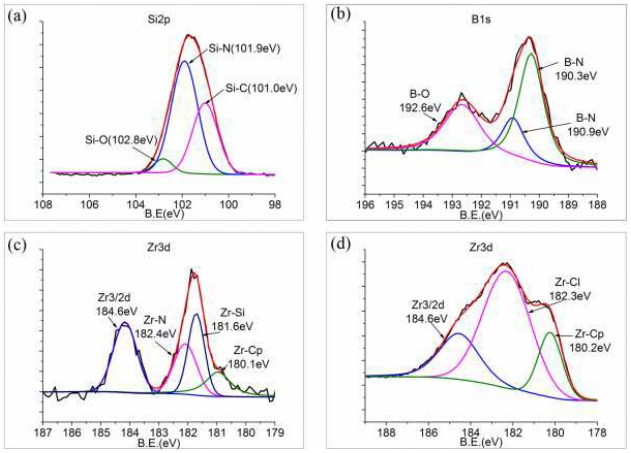

Fig. 1 Elemental X-ray photoelectron spectra of PBSZ-Zr10 (a for Si_{2p}, b for B_{1s}, c for Zr_{3d} in hybrid precursor and d for Zr_{3d} in Cp_2ZrCl_2)

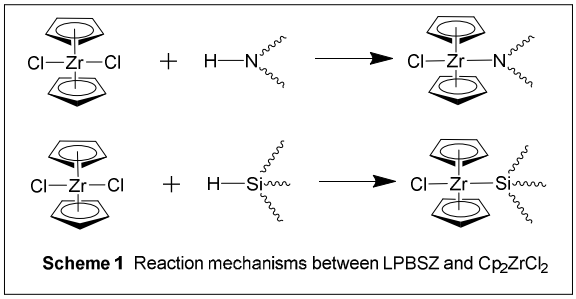

Scheme 1 Reaction mechanisms between LPBSZ and Cp_2ZrCl_2

The structure of the precursor polymer can be clearly confirmed by comparing the FT-IR spectra of the PBSZ/Cp_2ZrCl_2 precursor (Fig. 2a, b and c), PBSZ and Cp_2ZrCl_2 physical mixture (Fig. 2d), PBSZ (Fig. 2e) and Cp_2ZrCl_2 (Fig. 2f). The FT-IR spectra of hybrid precursor exhibit typical PBSZ characteristics. The broad peak at about 3429 cm^{-1} and the sharp peak at 1179 cm^{-1} are caused by N-H vibration [21], which become a little weaker as the weight ratio of Cp_2ZrCl_2 to LPBSZ increasing. The same phenomenon is also observed for Si-H vibration at 2125 cm^{-1} [21]. These results well confirm the reaction mechanism described previously (scheme 1). At 1015 cm^{-1} and 800 cm^{-1}, the peaks for C-H deformation in Cp rings [23] are observed in the spectrum of PBSZ/Cp_2ZrCl_2 hybrid precursor (Fig. 2(a)-(c)), which have a little shift compared with the peaks for PBSZ and Cp_2ZrCl_2 physical mixture (Fig 2(d)) and Cp_2ZrCl_2 (Fig 2(f)) at 1014 cm^{-1} and 809 cm^{-1}. These results indicate that Cp_2ZrCl_2 is successfully introduced into PBSZ.

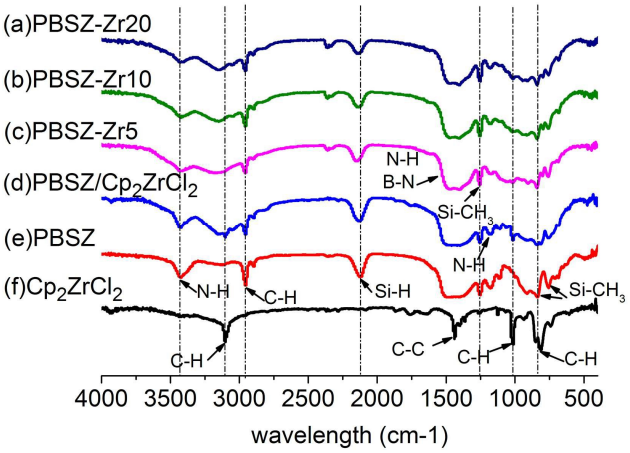

Fig. 2 FT-IR spectra of (a) PBSZ-Zr20, (b) PBSZ-Zr10, (c) PBSZ-Zr5, (d) PBSZ and Cp_2ZrCl_2 physical mixture, (e) PBSZ and (f) Cp_2ZrCl_2

The same conclusion can also be obtained from the ^{13}C NMR spectrum (Fig. 3). In comparison with the ^{13}C NMR spectrum of PBSZ (Fig. 3b), hybrid precursor (Fig. 3c~e) shows an additional resonance at about 112 ppm, which is caused by the Cp rings in the precursor. However, the chemical shift of Cp rings in hybrid precursor is a little different from the cyclopentadienyl signal at 115 ppm and 114 ppm of Cp_2ZrCl_2 (Fig. 3a). The difference of chemical shift can further confirm the introduction of Cp_2ZrCl_2 into PBSZ chains [23]. The peak at about 77 ppm is contributed to $DCCl_3$ which was used as the solvent. A broad peak at 0~8 ppm appears in the spectra of both PBSZ and hybrid precursor, which indicates that the carbon in PBSZ is mainly existed in the form of Si-CH_3.

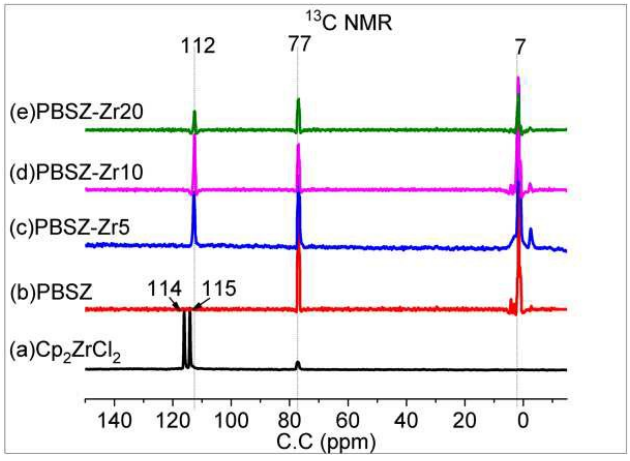

Fig. 3 13C NMR spectrums of (a) Cp_2ZrCl_2, (b) PBSZ, (c) PBSZ-Zr5, (d) PBSZ-Zr10 and (e) PBSZ-Zr20

The hybrid precursor was heated under a nitrogen atmosphere with the heating rate of 10 °C/min, and the weight change was recorded by TG-MS (Fig. 4). The ceramic yield of PBSZ, PBSZ-Zr5, PBSZ-Zr10 and PBSZ-Zr20 (1000 °C) in a N_2

atmosphere is 61.3 %, 60.0 %, 58.3 % and 57.6 %, respectively. This result indicates that the ceramic yield of PBSZ-Zr decreases slightly by the introduction of Cp_2ZrCl_2. The crosslinking between polymer chains occurs when the temperature is below 400 °C, accompanied by the escaping of oligomer. The polymer-to-ceramic conversion was observed at 400–800 °C with the release of CH_4 and NH_3. As the temperature went on, the NH_3 release of PBSZ and PBSZ-Zr10 both decreased, while the amount of CH_4 release reached a peak value at about 700 °C. Comparing the TG-MS graphs of PBSZ and PBSZ-Zr10 (Fig. 4), the CH_4 and NH_3 release by pyrolyzed PBSZ-Zr10 is a little weaker at 400–600 °C. Herein, the active groups in PBSZ-Zr10 reduced by Cp_2ZrCl_2 can suppress the release of CH_4 and NH_3. The further ceramic process completes above 800 °C with unchanged weight loss and few gas release.

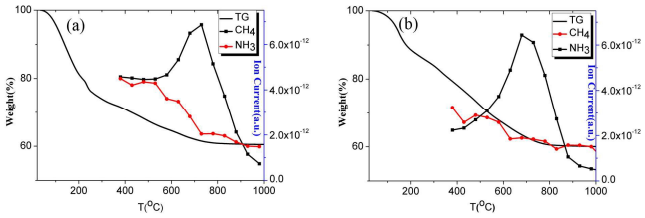

Fig. 4 TG-MS graphs of (a) PBSZ and (b) PBSZ-Zr10 pyrolyzed in a N2 atmosphere (Heat rate 10 K/min)

The ceramization of the hybrid precursor was also investigated by means of ^{29}Si MAS NMR (Fig. 5). The samples pyrolyzed at 400 °C (Fig. 5a and 5b) proves the presence of Si sites with mixed bonds (SiC_xN_{4-x}) in both PBSZ and PBSZ-Zr10. The signals at 0~12 ppm are assigned to SiC_3N sites (with sp^3 hybridized C) [24,25], and the signals at -20 ppm (highest intensity) and -39 ppm are attributed to $SiHCN_2$ and $SiCN_3$ centers [26,27], respectively. The $SiCN_3$ site signal intensity of PBSZ is stronger than the one of PBSZ-Zr10. This is because $SiCN_3$ sites are mainly formed by the reaction between N-H and Si-CH_3/Si-H, while the amount of N-H and Si-H groups was reduced by the reactant Cp_2ZrCl_2 in PBSZ-Zr10 through a chemical mechanism (scheme 1). The $SiHC_2N$ signal of PBSZ-Zr10 existed with an obvious high-field shift (shifting from -19 ppm in PBSZ to −21 ppm in PBSZ-Zr10), which is considered to be the reason for Zr bonded to the $SiHC_2N$ site coordination sphere [28].The presence of a weak signal at about -60 ppm is observed, which is assigned to SiN_3O centers [24]. Considering there is no oxygen in liquid polyborosilazane (LPBSZ) and Cp_2ZrCl_2, the oxygen may come from the oxygen and vapor in the air when transferring the products.

As the temperature went up to 800 °C, the SiC_3N sites signal disappeared completely (Fig. 5c and 5d), indicating the consumption of $Si(CH_3)_3$ groups in polymer and the complete polymer-to-ceramic translation process. The disappearance of SiC_3N sites could be explained by a free radical mechanism as below [29] (scheme 2). Herein, the SiC_3N sites translated to SiC_2N_2 and $SiCN_3$ through the radical mechanism, which is consistent with the increase of $SiCN_3$ signal at 800 °C. Contrary with $SiCN_3$ sites, the $SiHCN_2$ sites signal (at -20 ppm) becomes weaker obviously when the temperature went up to 800 °C (for both PBSZ and PBSZ-Zr10). The new signal at about -45 ppm is contributed to SiN_4 sites [24]. The decrease of $SiHCN_2$ sites and the increase of $SiCN_3$ and SiN_4 sites are related to the release of hydrogen and hydrocarbon (scheme 3) [24]. All the SiC_xN_{4-x} sites in PBSZ-Zr10 (Fig. 5d) have a high-field shift comparing with the one in PBSZ, but the change is not obviously. This interesting results indicate that Zr begin to release from the coordination sphere of the SiC_xN_{4-x} sites as the temperature increasing to 800 °C [28].

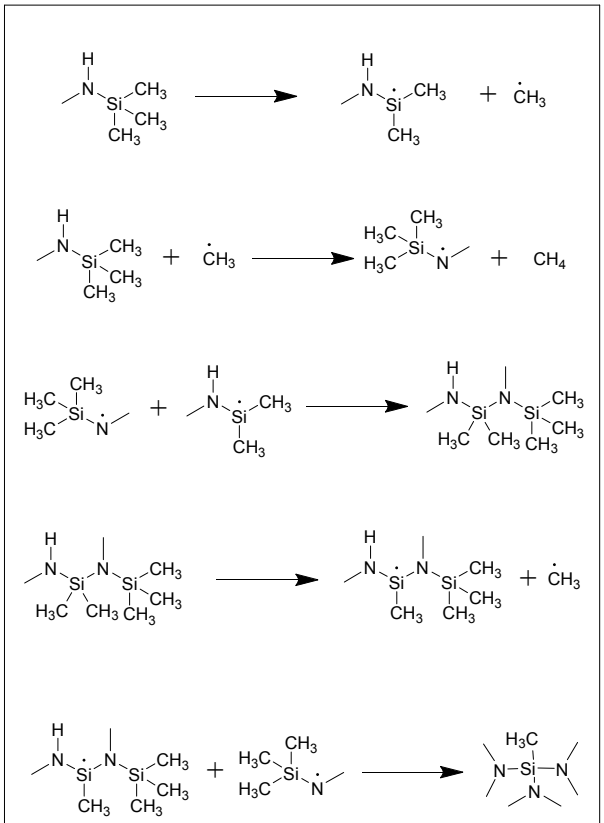

Scheme 2 Radical mechanism when pyrolyzed at about 800°C

The $SiHCN_2$ signal disappears completely when the temperature went up to 1200 °C (Fig. 5e and 5f), indicating the mineralization of precursor. $SiCN_3$ signal at -30 ppm and SiN_4 signal at -42 ppm only remained. The area of $SiCN_3$ signal is much larger than the area of SiN_4 signal in pyrolytic PBSZ-Zr10, which indicates that an obvious phase separation process occurs in SiBCN-Zr10 when the temperature elevated to 1200 °C [28]. Comparing with the signals of SiBCN, the signals belong to SiBCN-Zr10 are all broad ones. Considering the broadened of solid state nuclear magnetic resonance peak is related to the disorder of ceramic matrix, the introduction of Zr element may inhibit the crystallization of ceramic at high temperature [30].

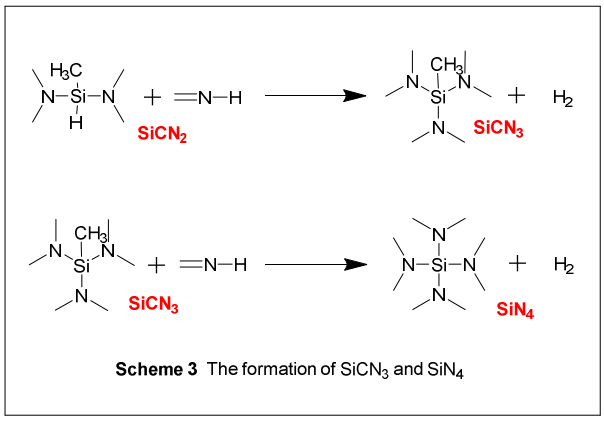

Scheme 3 The formation of $SiCN_3$ and SiN_4

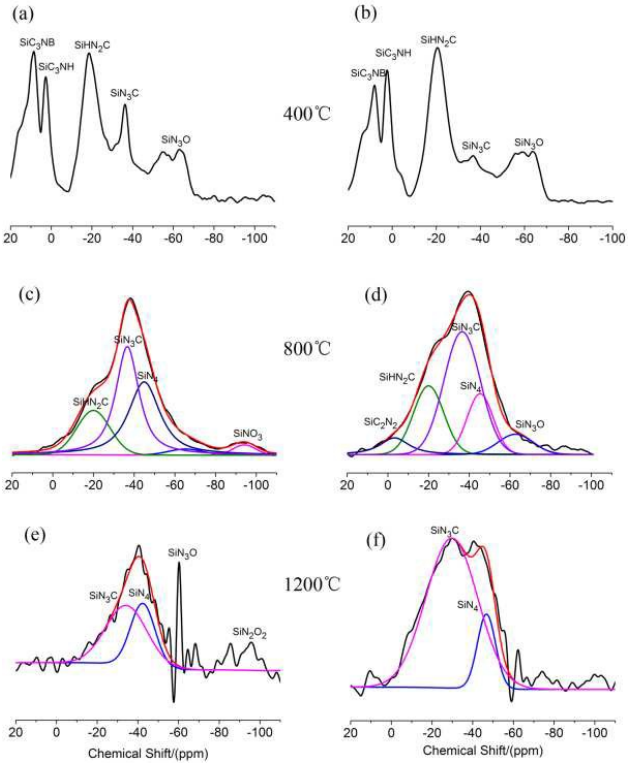

Fig. 5 The ^{29}Si MAS NMR spectrums of (a, c, e) PBSZ and (b, d, f) PBSZ-Zr10 pyrolyzed at different temperature

Chemical elemental analysis was taken to analyze the ceramic composition pyrolyzed at 1600 °C (Table 2). The hybrid precursor derived ceramic consist of silicon, zirconium, nitrogen, carbon, boron, and oxygen. It is worth mentioning that the zirconium or boron content of ceramic increases linearly with the increasing of the zirconium or boron content in hybrid precursor (Fig. 6). Therefore, zirconium and boron content in ceramic could be controlled by varying the zirconium and boron content in feed accurately. Moreover, due to the carbon in Cp escaping from the polymer chains at high temperature, the carbon content (at about 10 wt %) in ceramic changed few with the weight ratio of Cp_2ZrCl_2 to LPBSZ increasing.

Table 2 The elements composition of ceramic pyrolyzed at 1600 °C in an Ar atmosphere

Sample	Chemical analysis (wt %)					
	Si	B	N	C	Zr	O
PBSZ	30.0	10.1	44.7	9.6	0	4.0
PBSZ-Zr5	32.5	9.8	40.2	11.8	1.8	2.5
PBSZ-Zr10	34.9	8.2	39.9	11.5	2.3	2.2
PBSZ-Zr20	35.8	7.6	35.2	12.1	4.1	3.5

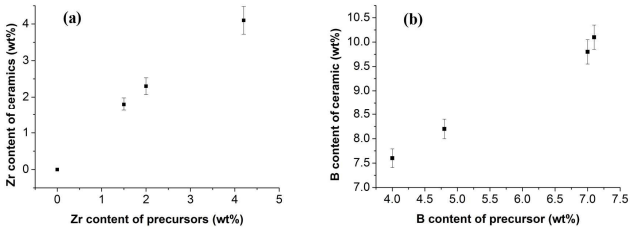

Fig. 6 The relationship of element content between ceramics and precursor (a, Zr content; b, boron content)

Fig. 7a shows the XRD patterns of the PBSZ-Zr10 pyrolyzed at different temperatures. SiBCN-Zr10 ceramic can remain amorphous at 1200 °C. When the temperature went up to 1600 °C, peaks at 33.5° (111), 38.8° (200), 56.0° (220) and 66.8° (311) appeared, indicating the formation of Zr_2CN (JPCDS Card No. 65-8779) crystalline phase. Meanwhile, hexagonal Si_3N_4 (JPCDS Card No. 33-1160) and ZrC (JPCDS Card No. 65-8832) crystalline phases were also detected. At 1800 °C, Zr_2CN peaks disappeared, while the additional peaks for ZrB_2 (JPCDS Card No. 65-8704) was detected, which indicates the transformation from Zr_2CN to ZrB_2. The disappearance of hexagonal Si_3N_4 and the detective of SiC and Si shows that the hexagonal Si_3N_4 phases decomposed to SiC and Si through a thermal decomposition process. As the Cp_2ZrCl_2 content in reactant increasing, the intensity of Zr_2CN peaks at 1600 °C significantly increased (Fig. 7b).

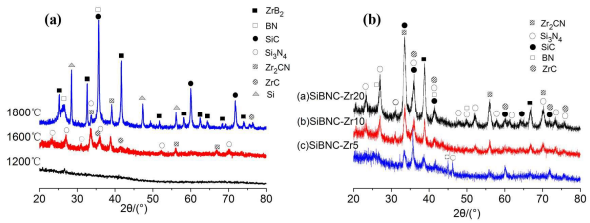

Fig. 7 The XRD patterns for SiBCN-Zr10 pyrolyzed at 1200 °C, 1600 °C and 1800 °C (a) and for SiBCN-Zr5, SiBCN-Zr10 and SiBCN-Zr20 pyrolyzed at 1600 °C (b)

The microstructural evolution of Zr-content samples at high temperature was characterized by transmission electron microscopy (TEM). As for SiBCN-Zr10 ceramic annealed at 1200 °C, nanoparticles (the dark area of Fig. 8a) with sizes of ca.

10 nm embedded within amorphous SiBCN based matrix were observed. As the temperature went up to 1600 °C, a partial phenomenon of the nanoparticles had taken place (Fig 8b). From high resolution transmission electron microscopy (HRTEM) graph (Fig 8d), we can get that the lattice fringe spacing of the nanoparticles is 0.26 nm, corresponding to the (111) lattice plane of Zr_2CN (JPCDS Card No. 65-8779). Meanwhile, the lattice fringe with a spacing of about 0.34 nm was also observed, which belongs to the BN or BCN crystallization.

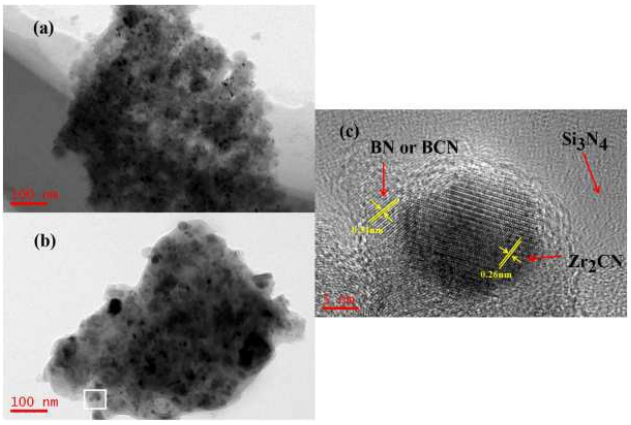

Fig. 8 TEM graphs for SiBCN-Zr10 annealed at (a) 1200 °C and (b) 1600 °C; (c) HRTEM graph for SiBCN-Zr10 annealed at 1600 °C

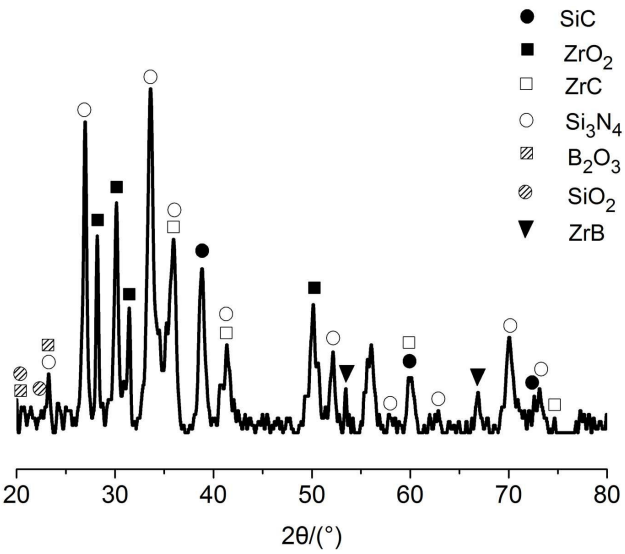

Fig. 9 The XRD pattern of SiBCN-Zr20 ceramic after oxidation

Zr-content SiBCN ceramic after annealed at 1600 °C was treated at 1550 °C in an air atmosphere to test the oxidation resistance. The weight retention of SiBCN ceramic was only 87.5 %, while the weight retention of SiBCN-Zr ceramics reached nearly 100% (97.5 %, 98.1 % and 99. 4 % for SiBCN-Zr5, SiBCN-Zr10 and SiBCN-Zr20, correspondingly). Thus, we believe that the oxidation resistance of SiBCN ceramic was greatly improved by the introduction of Zr element. The XRD pattern (Fig. 9) of SiBCN-Zr20 ceramic after oxidation test shows that although the oxidation phases such as ZrO_2, B_2O_3 and SiO_2 are detected, the mainly phases such as Zr_2CN, Si_3N_4, ZrC and SiC still remained. The ceramic powder which is obtained by smashing the oxidation tested SiBCN-Zr20 ceramic, was analyzed by EDS(Fig. 10). The results show that the oxygen content on the ceramic interface (1#) is 12.72 wt %, which is far greater than the average value obtained by Oxygen/Nitrogen Analyzer (2.90 wt %). However, the oxygen content in the fracture (2#) is only 1.26 wt %, which indicates the oxidation reaction taken place only on the interface of the ceramic.

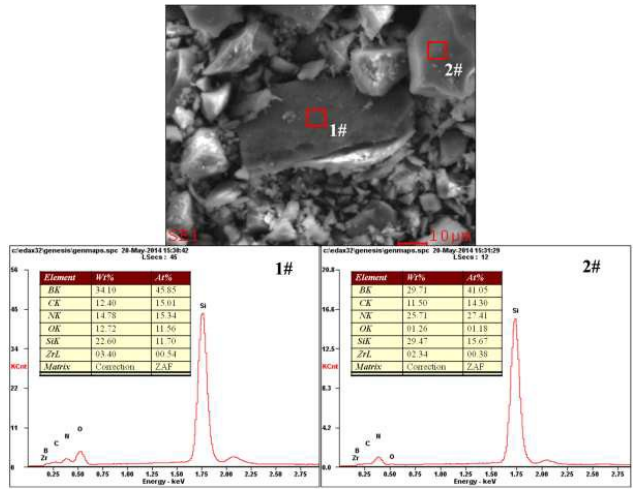

Fig. 10 EDS spectra of SiBCN-Zr20 ceramic powder after oxidation

Former studies have shown that the oxidation rate of silicon-based polymer-derived ceramics depends on two major factors: the diffusivity of oxygen through the silica overlayer and the difference in the chemical potential of oxygen at the surface and at the oxide-substrate interface [31]. The chemical potential at the ceramic surface is constant, which is fixed by the atmosphere, but the potential at the interface mainly depends on the reaction $2C + O_2 \rightarrow 2CO$ [32]. So in this way, a lower activity of carbon at the ceramic interface can low the driving force for oxidation thereby increasing the weight retention of the SiBCN-Zr. EDS results have shown that the N content at the SiBCN-Zr20 ceramic fracture was 25.71 wt %, which decreased largely to 14.78 wt % at ceramic interface. In the SiBCN ceramic matrix, the N atoms were mainly bonded with Si to form Si_3N_4, thus the decrease of N content at ceramic interface makes more amount of Si to bond with free carbon, which lowed the activity of carbon at the ceramic interface. However, owing to the limitation of our work, the relationship between the introduction of Zr element and the decrease of N content was not clear.

Conclusions

Zirconium-contained polyborosilazane (PBSZ-Zr) was synthesized by chemical modification of a liquid polyborosilazane (LPBSZ) with Cp_2ZrCl_2. PBSZ-Zr hybrid precursor with different content of Zr is synthesized, and the structure of hybrid precursors was characterized by FT-IR and ^{13}C NMR. The polymer to ceramic process of PBSZ-Zr was identified by TG-MS and ^{29}Si MAS NMR. PBSZ-Zr hybrid precursor was converted into multinary ceramic when heated above 800 °C in a N_2 atmosphere, and the ceramic yield at 1000 °C was 57.6%~60.3%. SiBCN-Zr ceramic can remain amorphous at 1200 °C, and the Zr_2CN nanoparticles with sizes of ca. 10 nm were embedded within amorphous SiBCN-based matrix. As the temperature went up to 1600 °C, a partial phenomenon of the nanoparticles had taken place. The oxidation resistant of SiBCN-Zr was remarkably superior to SiBCN due to the low activity of free carbon at the ceramic interface. This work provided a novel polymer-derived ceramic method for the synthesis of Si-B-N-C-Zr ceramic, which could be easily applied in the synthesis of Si-B-N-C-Hf, Si-B-N-C-Ta and other multinary ceramics for ultra-high-temperature applications.

Acknowledgements

This work is supported by the National Natural Science Foundation of China (51203184), the Fund of the Science and Technology on Advanced Ceramic Fibers and Composites Laboratory (9140C820207130C82278), and the Support Fund of the Aerospace Science & Technology.

Notes and reference

1 R. Riedel, A. Kienzle and W. Dressler, *Nature*, 1996, **382**, 796.
2 P. Baldus, M. Jansen and D. Sporn, *Science*, 1999, **285**, 699.
3 M. Jansen, B. Jäschke and T. Jäschke, *Springer Berlin Heidelberg*, 2002: 137.
4 D. W. Johnson, A. G. Evans and R. W. Goettler, *National Research Council* , 1998, 22.
5 M. M. Opeka, I. G. Talmy and J. A. Zaykoski, *J. Mater. Sci.*, 2004, **39**, 5887.
6 D. M. Van Wie, D. G. Drewry Jr and D. E. King, *J. Mater. Sci.*, 2004, **39**, 5915.
7 W. G. Fahrenholtz, G. E. Hilmas and I. G. Talmy, *J. Am. Ceram. Soc.*, 2007, **90**, 1347.
8 Y. Yan, Z. Huang and X. Liu, *J. Sol-Gel Sci. Technol.*, 2007, **44**, 81.
9 F. Monteverde and A. Bellosi, *J. Eur. Ceram. Soc.*, 2005, **25**, 1025.
10 W. C. Tripp, H. H. Davis and H. C. Graham, *Am. Ceram. Soc. Bull.*, 1973, **52**, 612.
11 F. Monteverde and L. Scatteia, *J. Am. Ceram. Soc.*, 2007, **90**, 1130.
12 C. Bartuli, T.Valente and M. Tului, *Surf. Coat. Tech.*, 2002, **155**, 260.
13 F. Monteverde, A. Bellosi and S. Guicciardi. *J. Eur. Ceram. Soc.*, 2002, **22**, 279.
14 I. G. Talmy, J. A. Zaykoski and M. M. Opeka, *J. Am. Ceram. Soc.*, 2008, **91**, 2250.
15 G. Li, W. Han and B. Wang, *Mater. Des.,* 2011, **32**, 401.
16 D. Zhao, H. Hu, C. Zhang, Y. Zhang and J. Wang, *J. Mater. Sci.*, 2010**, 45**, 6401.
17 M. Fan, E. N. Duesler, J. F. Janik and R.T. Paine, *J. Inorg. Organomet. Polym. Mater.*, 2007, **17**, 423.
18 C. J. Liu, L. H. Liu, S. Y. Yang, W. Gao and Z. M. Xie, *Chin. Chem. Lett.,* 2002, **13**, 1225.
19 L. H. Liu, C. J. Liu, S. Y. Yang, W. Gao and Z. M. Xie, *Chin. J. Polym. Sci.*, 2003, **21**, 99.
20 A. M. Tsirlina, G. I. Shcherbakovaa, E. K. Florinaa, N. A. Popovaa and S. P. Gubinbm, *J. Eur. Ceram. Soc.*, 2002, **14**, 2577.
21 Y. Tang, J. Wang and X. D Li, *J. Appl. Polym. Sci.*, 2008, **110**, 921.
22 R. Bhandavat, A. Feldman and C. Cromer, *Appl. Mater. Interfaces*, 2013, **5**, 2354.
23 Z. J. Yu, L. Yang and J. Y. Zhan, *J. Eur. Ceram. Soc.*, 2012, **32**, 1291.
24 E. Ionescu, B. Papendorf and H. J. Kleebe, *J. Eur. Ceram. Soc.*, 2012, **32**, 1873.
25 L. M. Ruwisch, P. Durichen and R. Riedel, *Polyhedron*, 2000, **19**, 323.
26 C. Gerardin, F. Taulelle and D. Bahloul, *J. Mater. Chem.*, 1997, **7**, 117.
27 J. Bill, J. Seitz and G. Thurn, *Phys. Stat. Sol.*, 1998, **166**, 269.
28 J. Yuan, S. Hapis, R. Riedel and E. Ionescu, *Inorg. Chem.*, 2014, **53**: 10443.
29 R. Corriu, D. Leclercq and P. H. Mutin, *Chem. Mater.*, 1992, **4**, 711.
30 M. A. Schiavon, G. D. Soraru and I. V. P. Yoshida, *J. Non-Cryst. Solids*, 2002, **304**, 76.
31 A. Saha, S. R. Shah and R. Raj, *J. Am. Ceram. Soc.*, 2004, **87**, 1556.
32 S. Modena, G. D. Soraru, Y. Blum and R. Raj, *J. Am. Ceram. Soc.*, 2005, **88**, 339.